DOI: 10.1002/ejic.201100824

A Quest for Ligand-Unsupported Li^+–π Interactions in Mono-, Di-, and Tritopic Lithium Arylborates

Daniel Franz,[a] Alireza Haghiri Ilkhechi,[a] Michael Bolte,[a] Hans-Wolfram Lerner,[a] and Matthias Wagner*[a]

Keywords: Lithium / Polyanions / Borates / Bridging ligands / Coordination modes

The lithium salts of selected mono-, di-, and tritopic arylborates have been synthesized and their solid-state structures have been analyzed by X-ray crystallography with focus on the occurrence of Li^+–aryl π interactions. The solvated salts of the monotopic arylborate $[Li(thf)_4][(p\text{-}BrC_6H_4)BPh_3]$ as well as the ditopic borates $[Li(12\text{-crown-}4)_2]_2[p\text{-}C_6H_4(BMe_3)_2]$ and $[Li(tetraglyme)]_2[p\text{-}C_6H_4(BPh_3)_2]$ exist as solvent-separated ion pairs in the crystal lattice. The attachment of two moderately coordinating monohydridoborate functionalities on a benzene ring leads to Li^+–hydride interactions. In the case of $[Li(thf)_3]_2[p\text{-}C_6H_4\{9\text{-BBN(H)}\}_2]$ [9-BBN(H) = 9-borabicyclo[3.3.1]nonane], this additional attractive force is not sufficient to promote Li^+–aryl π interactions, however, the 1,2-dimethoxyethane (DME) solvate $[Li(dme)_2]_2[p\text{-}C_6H_4\{9\text{-BBN(H)}\}_2]$ shows a remarkably short contact between the Li^+ cation and the adjacent phenylene *ipso* carbon atom [Li–C 2.366(2) Å]. The targeted structural motif of Li^+–arene η^6 coordination was finally observed in the solid-state structures of the tritopic borates $[\{Li(12\text{-crown-}4)_2\}_2\text{-}Li(thf)][1,3,5\text{-}C_6H_3(BMe_3)_3]$ and $[\{Li(thf)_2\}_2Li][1,3,5\text{-}C_6H_3(BH_3)_3]$. In the latter complex, an extensive network of Li–H–B bonds is observed in addition to the Li^+–π interaction.

Introduction

In the field of organolithium chemistry, the major focus has long been on the lithium–carbon σ bond, as this type of compound is widely used for organyl group transfer reactions.[1] In contrast, the important interaction between Li^+ and the negative charge density of organic π systems (e.g. alkenes, alkynes, arenes), which is one of the strongest noncovalent binding forces, came to be appreciated much more recently.[2–5] Today, it is undisputed that Li^+ cation–π interactions are relevant for numerous applications, e.g. as a conformation-controlling tool in various regio- and stereoselective syntheses[6–11] and for the intercalation of lithium between graphite layers in lithium-ion batteries.[12]

Experimental and theoretical gas-phase binding energies indicate that alkali metal ion–π interactions tend to follow a classical electrostatic trend (i.e. $Li^+ > Na^+ > K^+ > Rb^+$) because the Coulomb attraction between the cation and the quadrupolar moment of the aromatic component adds an important contribution to the overall binding energy.[2] In solution or the solid state, however, this sequence can be modified by coordinated solvent molecules and/or crystal packing forces. The corresponding structural information is notoriously difficult to obtain given that the majority of organolithium reagents are only soluble in donor solvents, which are tough competitors with organic π systems for Li^+ coordination. In the quest for solid-state evidence, various classes of compounds have been investigated. They can roughly be divided into four categories: Category (1) comprises lithium salts of fused aromatics such as $[Li(tmeda)]_2[C_{10}H_8]$ (tmeda = *N*,*N*,*N*′,*N*′-tetramethylethylene-1,2-diamine), which contains two $[Li(tmeda)]^+$ ions coordinated to opposite faces of the organic plane.[13] Category (2) includes species in which Li^+–π interactions are supported by intramolecular chelation with (anionic) σ donor functionalities.[14] Category (3) consists of aryllithium compounds that show Li^+–π coordination in addition to Li–C σ bonds.[15] Examples are Lewis base-free phenyllithium $([LiPh]_n)$,[16] mesityllithium $([LiMes]_n)$,[17] and 2,4,6-triisopropylphenyllithium $([LiTrip]_4)$;[18] several heterodinuclear lithium "ate" complexes fall into a similar category, e.g. $[Cu_2Li_2Mes_4]$[19] and $[Li(OEt_2)]_4[FePh_4]$[20]. Category (4) comprises compounds in which π interactions are established between Li^+ and neutral arenes in the absence of a chelating side arm, e.g. $[Li(C_6H_6)][2,6\text{-}Trip_2C_6H_3]$,[21] $[Li(C_6H_6)][Sn\{SiMe(tBu)_2\}_3]$,[22] and $[Li(C_6H_6)][B(C_6F_5)_4]$.[23]

Our own interest in cation–π interactions was sparked by the serendipitous finding that ferrocene reacts with $GaCl_3$ to give $[(C_5H_5)_2Fe][GaCl_4]$ together with the crystalline Ga^I multiple-decker sandwich complex **I** (Figure 1).[24] By attaching anionic (pyrazol-1-yl)borate substituents to both cyclopentadienyl rings of ferrocene (**II**; Figure 1),[25–27] our group has achieved the targeted synthesis of multiple-decker sandwich complexes of ferrocene with the complete

[a] Institut für Anorganische Chemie, J. W. Goethe-Universität Frankfurt,
Max-von-Laue-Strasse 7, 60438 Frankfurt (Main), Germany
Fax: +49-69-798-29260
E-mail: Matthias.Wagner@chemie.uni-frankfurt.de

Supporting information for this article is available on the WWW under http://dx.doi.org/10.1002/ejic.201100824.

series of alkali metals (M^+ = Li^+–Cs^+).[28] In these compounds, the purpose of the chelating (pyrazol-1-yl)borate moiety was to increase the electrostatic attraction of the alkali-metal ion and to use the directing effect of the nitrogen lone pair to place the ion over the centroid of the π face. The Lewis basic pyrazol-1-yl substituent may be replaced by a phenyl ring: the lithium borate **III** (Figure 1) contains the Li^+ cations nested in V-shaped spaces created by a cyclopentadienyl ring and a phenyl substituent.[29]

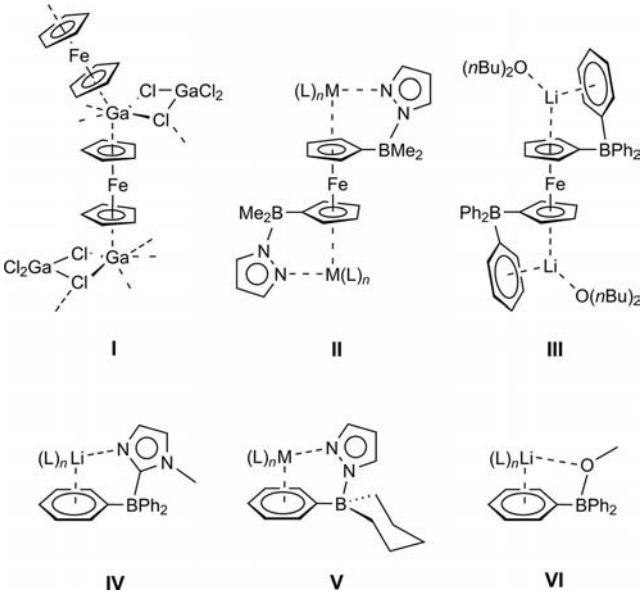

Figure 1. The ligand-unsupported Ga^I–ferrocene multiple-decker sandwich complex **I**; alkali-metal ion–ferrocene multiple-decker sandwich complexes **II** (M^+ = Li^+–Cs^+) and **III** bearing a chelating, anionic side arm; ligand-supported metal ion–benzene π complexes **IV**, **V** (M^+ = K^+, Tl^+), and **VI**.

Compound **III** can equally be viewed as a Li^+–benzene π complex. We therefore conclude that the attachment of anionic borate substituents may help to stabilize a broader variety of Li^+–π interactions. This conclusion is supported by the solid-state structures of **IV**,[30] **V**,[31] and **VI**,[32] which all feature Li^+–benzene π coordination (Figure 1). In **IV**–**VI**, the desired structural motif is still enforced by a chelating side arm. However, η^6 coordination of the Li^+ ion in $\{Li[Et_3GeBPh_3]\}_n$[33] shows that, at least in the absence of donor solvents, it suffices to attach a negative charge to the benzene ring. In some respect, compounds **IV**–**VI** and $\{Li[Et_3GeBPh_3]\}_n$ are reminiscent of category (3) "ate" complexes.

Given this background, we now provide a critical survey of the syntheses and key structural motifs of lithium salts containing benzene derivatives with one, two, or three anionic $[–BR_3]^–$ substituents (R = H, alkyl, aryl). We will focus on the competition between ethereal solvents and the respective π systems for Li^+ coordination as a function of the number of negatively charged substituents attached to the benzene ring. Anions of the form $[ArylBR_3]^–$ can possess ligand properties similar to those of the $[C_5H_5]^–$ ring as both species are monoanionic, six-electron donors. The $[C_5H_5]^–$ anion is among the most popular π donor ligands in coordination chemistry,[1] and single- as well as multiple-decker sandwich complexes are known.[34]

Results and Discussion

In contrast to other negatively charged functional groups (e.g. $[–SO_3]^–$), the borate substituent $[–BR_3]^–$ (R = H, alkyl, aryl) does not possess electron lone pairs able to act as σ donor ligands, but merely puts an attractive point charge in close vicinity to the aromatic π system. In order to keep the steric demand as low as possible, we initially employed $[–BH_3]^–$ moieties {e.g. $[Li(thf)_2]_2[m\text{-}C_6H_4(BH_3)_2]$,[35] $[Li(thf)_2]_2[p\text{-}C_6H_4(BH_3)_2]$,[35] $[Li(OEt_2)_2][FcBH_3]$ (Fc = ferrocenyl, thf = tetrahydrofuran)}[36] but had to recognize that the Li^+ ions tended to coordinate to the peripheral hydride substituents rather than to the benzene or cyclopentadienyl π faces.

Dianionic Benzene Derivatives

Given the experiences discussed above, we decided to replace the hydride by methyl substituents and turned our attention to a benzene ring equipped with two $[–BMe_3]^–$ groups in mutually *para* positions (Li_2[**2**], Scheme 1). The dilithium salt Li_2[**2**] is readily accessible from *p*-bis(dibromoboryl)benzene (**1**)[37] and six equivalents of MeLi in Et_2O/toluene at –78 °C. Despite numerous efforts to grow X-ray quality crystals of Li_2[**2**] in the absence of strongly coordinating chelators, we were only able to obtain the 12-crown-4 (12-c-4) adduct $[Li(12\text{-}c\text{-}4)_2]_2$[**2**] as single crystals. Each Li^+ ion in $[Li(12\text{-}c\text{-}4)_2]_2$[**2**] is sandwiched between two 12-c-4 molecules and therefore establishes no close contacts to the anion {see Supporting Information for more details on the synthesis, NMR spectroscopic data, and the crystal structure of $[Li(12\text{-}c\text{-}4)_2]_2$[**2**]}.

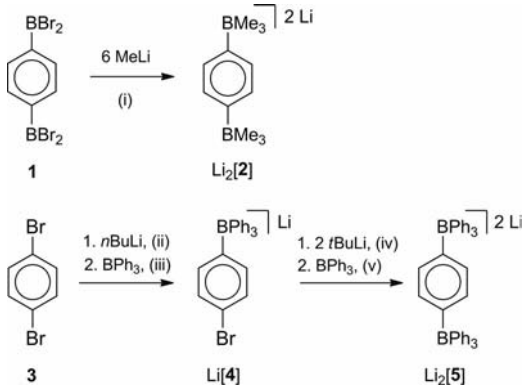

Scheme 1. Synthesis of Li_2[**2**] and Li_2[**5**]. (i) Et_2O/toluene, –78 °C → room temp. (ii) Et_2O/hexane, –78 °C → –50 °C. (iii) Et_2O/hexane/toluene, –78 °C → room temp. (iv) THF/pentane, –78 °C → –50 °C. (v) THF/pentane/Et_2O, –78 °C → room temp.

The methyl groups were next exchanged for phenyl rings (Li_2[**5**], Scheme 1), because (i) this alters the solubility of the lithium salt and (ii) the new anion provides V-shaped

cavities between the phenylene bridge and the phenyl substituents, which are ideally suited to host a Li^+ ion (cf. the analogous solid-state structure of **III**, Figure 1). The synthesis of Li_2[**5**] proceeded by a sequential lithium-halogen exchange on *p*-dibromobenzene with *n*BuLi and *t*BuLi, respectively, and trapping of the intermediates with BPh_3.[38] We isolated both monoborate Li[**4**] and diborate Li_2[**5**] as single crystals as THF adducts, $[Li(thf)_4]$[**4**] and $[Li(thf)_4]_2$[**5**], and as the tetraglyme adduct, $[Li(tetraglyme)]_2$-[**5**]. Similar to $[Li(12\text{-c-}4)_2]_2$[**2**], X-ray crystallography of $[Li(thf)_4]$[**4**], $[Li(thf)_4]_2$[**5**], and $[Li(tetraglyme)]_2$[**5**] revealed fully solvent-separated ion pairs and no Li^+–π interactions (see SI for more details on the syntheses, NMR spectroscopic data, and the crystal structures of these compounds).

Trihydridoborates have a tendency to bind Li^+ ions, and the most abundant coordination mode is η^2.[35,36] Given this background, we next chose the ditopic monohydridoborate Li_2[**8**] (Scheme 2) as the new target system because (i) the moderately coordinating character of the hydridoborate moiety should exert a directing effect that increases the probability for π interaction between Li^+ and the phenylene ring and (ii) the cyclic structure of the 9-borabicyclo[3.3.1]-nonane (9-BBN) fragment should help to avoid substituent scrambling, and its lipophilicity should increase the solubility of the lithium salt in less polar solvents.

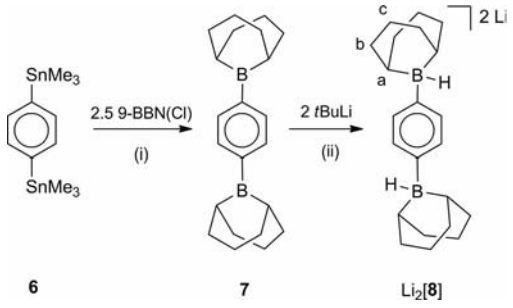

Scheme 2. Synthesis of Li_2[**8**]. (i) Toluene, 120 °C, 24 h. (ii) THF/hexane/pentane, –78 °C → room temp., 12 h.

The synthesis of Li_2[**8**] started from *p*-bis(trimethylstannyl)benzene (**6**),[39] which is transformed into the triorganylborane **7** by the reaction with 9-BBN(Cl)[40] in toluene at 120 °C (see SI for more details on the synthesis, NMR spectroscopic data, and the crystal structure of **7**). Subsequent treatment of **7** with two equivalents of *t*BuLi at –78 °C gave Li_2[**8**] in a clean conversion (see ref.[41] for related hydride-transfer reactions). The successful generation of a monohydridoborate was proven by an upfield shift of the $^{11}B\{^1H\}$ resonance from 82.5 ppm ($h_{1/2}$ = 600 Hz) in **7** to –11.4 ppm ($h_{1/2}$ = 60 Hz) in Li_2[**8**]. In the ^1H-coupled $^{11}B\{^1H\}$ NMR spectrum, the latter signal appears as a doublet with a coupling constant of $^1J_{BH}$ = 60 Hz {cf. Li[9-BBN(Ph)(H)]: $\delta(^{11}B)$ = –13.9 ppm, d, $^1J_{BH}$ = 55 Hz}.[41] Moreover, because of the reduced symmetry as a result of hydride addition, the BBNC-b and BBNC-c carbon atoms of Li_2[**8**] (Scheme 2) each give rise to two resonances, whereas only one set of ^{13}C NMR signals is observed for the two 9-BBN fragments in the more symmetric **7**. A similar ^{13}C NMR resonance pattern as observed for the 9-BBN substituent of Li_2[**8**] has been described for Na[9-BBN(Et)(H)].[42]

Li_2[**8**] was crystallized from 1,2-dimethoxyethane (DME) as well as from THF. The molecular structure of $[Li(dme)_2]_2$[**8**] is presented in Figure 2.

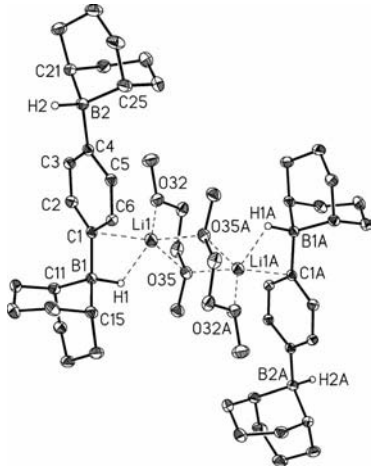

Figure 2. Molecular structure of $[\{Li(dme)\}\{\mathbf{8}\}]_2^{2-}$; displacement ellipsoids are at 30% probability. All H atoms attached to carbon atoms are omitted for clarity. Selected bond lengths [Å], atom···atom distances [Å], and bond and torsion angles [°]: Li(1)–O(32) 1.966(2), Li(1)–O(35) 2.346(2), Li(1)–O(35A) 2.082(2), Li(1)–C(1) 2.366(2), Li(1)–H(1) 1.818(15), Li(1)···B(1) 2.512(2), B(1)–C(1) 1.637(2), B(1)–C(11) 1.630(2), B(1)–C(15) 1.635(2), B(2)–C(4) 1.630(2), B(2)–C(21) 1.638(2), B(2)–C(25) 1.634(2); O(32)–Li(1)–O(35) 80.1(1), O(32)–Li(1)–O(35A) 100.9(1), Li(1)–H(1)–B(1) 109.5(9), C(11)–B(1)–C(15) 104.6(1), C(21)–B(2)–C(25) 104.6(1); Li(1)–H(1)–B(1)–C(1) 5.3(9). Symmetry transformation used to generate equivalent atoms: A: $-x + 1, -y + 1, -z + 2$.

The crystal lattice contains two kinds of Li^+ ions: Li(2) (not shown in Figure 2) is coordinated by three DME molecules in a distorted octahedral fashion. Li(1), which is part of a centrosymmetric dimer $[\{Li(dme)\}\{\mathbf{8}\}]_2^{2-}$, is chelated by only one DME ligand. In addition, it binds to one B*H* moiety of its counteranion [Li(1)–H(1) 1.818(15) Å; Li(1)···B(1) 2.512(2) Å] and to the DME oxygen atom of the symmetry-related monomer within the dimer [Li(1)–O(35A) 2.082(2) Å]. Most importantly, there is also a close contact between Li(1) and the adjacent phenylene *ipso* carbon atom. The corresponding bond length Li(1)–C(1) 2.366(2) Å agrees with the sum of the half-thickness of benzene (1.7 Å)[3] and the ionic radius[43] of four-coordinate Li^+ (1.7 Å + 0.60 Å = 2.30 Å). In line with the proposed bonding interaction between Li(1) and C(1), the Li(1)–H(1)–B(1) bond angle is comparatively small [109.5(9)°] and the torsion angle Li(1)–H(1)–B(1)–C(1) 5.3(9)° is close to 0°.

The Li^+–π interaction in $[\{Li(dme)\}\{\mathbf{8}\}]_2^{2-}$ is very sensitive to changes in the ligand sphere of the Li^+ cations. The monomeric and centrosymmetric THF solvate $[Li(thf)_3]_2$[**8**] (Figure 3), in which each Li^+ cation is also surrounded by three oxygen donors, still features a Li–H bond [Li(1)–H(1) 1.78(2) Å; Li(1)···B(1) 2.729(4) Å], but the Li(1)···C(1) distance is elongated to 3.062(5) Å. Moreover, the Li(1)–H(1)–

B(1) bond angle is stretched by almost 20° to a value of 128(2)° and the Li(1)–H(1)–B(1)–C(1) torsion angle is equal to –53(2)° rather than 5.3(9)° in $[\{Li(dme)\}\{\mathbf{8}\}]_2^{2-}$.

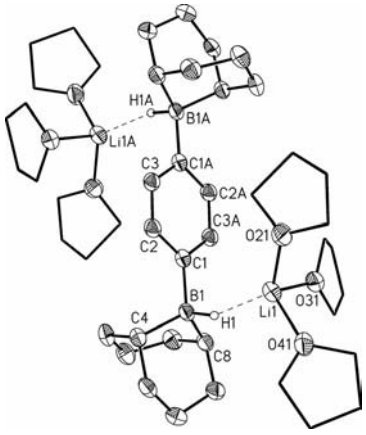

Figure 3. Molecular structure of $[Li(thf)_3]_2$[**8**]; displacement ellipsoids are at 30% probability. H atoms attached to carbon atoms are omitted for clarity. Selected bond lengths [Å], atom···atom distances [Å], and bond and torsion angles [°]: Li(1)–O(21) 1.939(5), Li(1)–O(31) 1.956(5), Li(1)–O(41) 1.983(5), Li(1)···C(1) 3.062(5), Li(1)–H(1) 1.78(2), Li(1)···B(1) 2.729(4), B(1)–C(1) 1.626(3), B(1)–C(4) 1.638(3), B(1)–C(8) 1.633(3); Li(1)–H(1)–B(1) 128(2), C(4)–B(1)–C(8) 104.3(2); Li(1)–H(1)–B(1)–C(1) –53(2).

Trianionic Benzene Derivatives

We continued our investigation with the trisubstituted Li_2[**2**]-analogue Li_3[**10**] (Scheme 3).

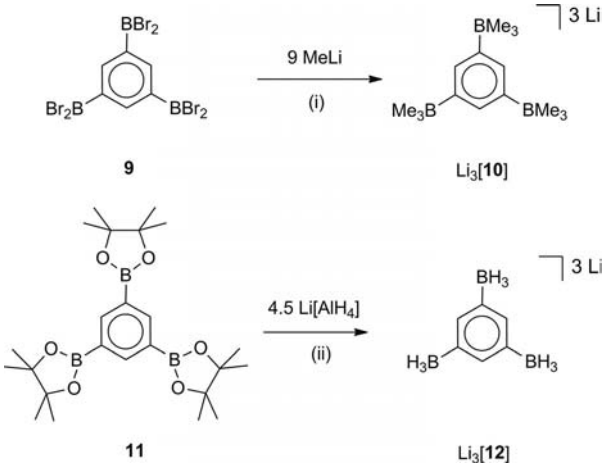

Scheme 3. Synthesis of Li_3[**10**] and Li_3[**12**]. (i) Et_2O/toluene, –78 °C → room temp. (ii) Et_2O, –30 °C → room temp.

Li_3[**10**] was obtained from 1,3,5-tris(dibromoboryl)benzene[37] and nine equivalents of MeLi in Et_2O/toluene at low temperature.

The $^{11}B\{^1H\}$ NMR spectrum of Li_3[**10**] is characterized by a resonance at –17.3 ppm, typical of four-coordinate boron centers.[44] The integral ratio between the C_6H_3 proton resonance and the $B(CH_3)$ signal is 1:9, which is in line with the introduction of three methyl substituents at each boron atom. The $B(CH_3)$ resonance appears in the ^{13}C NMR spectrum at 20.0 ppm as a 1:1:1:1 quartet with a coupling constant $^1J_{BC}$ of 40 Hz.

In order to ensure maximum comparability with $[Li(12\text{-}c\text{-}4)_2]_2$[**2**] and thereby to extract the structure determining effect of the third negative substituent, we crystallized Li_3[**10**] under the same conditions as Li_2[**2**], i.e. from THF/Et_2O in the presence of excess 12-c-4. The crystals obtained had the composition $[\{Li(12\text{-}c\text{-}4)_2\}_2Li(thf)]$[**10**]. Similar to $[Li(12\text{-}c\text{-}4)_2]_2$[**2**], the X-ray crystal structure of $[\{Li(12\text{-}c\text{-}4)_2\}_2$-Li(thf)][**10**] showed two Li^+ ions embedded between two 12-c-4 ligands. The third Li^+ ion, however, binds to the C_6H_3 bridge of the borate anion in an η^6 mode with Li(2)–C distances ranging between 2.250(7)–2.307(7) Å (Figure 4). The distance between Li(2) and the centroid of the aromatic ring, Li(2)–COG, is 1.784 Å. Depending on the level of theory, Li–COG distances of 1.879[45] and 1.842 Å[46] have been calculated for the Li^+–benzene complex in the gas phase. Thus, the Li(2)–COG contact in $[\{Li(12\text{-}c\text{-}4)_2\}_2Li(thf)]$[**10**] is remarkably close. One THF molecule completes the ligand sphere of Li(2). The corresponding Li(2)–O(61) bond length of 1.891(6) Å is significantly shorter than the Li–O bond lengths in $[Li(thf)_3]_2$[**8**] [i.e. 1.939(5)–1.983(5) Å].

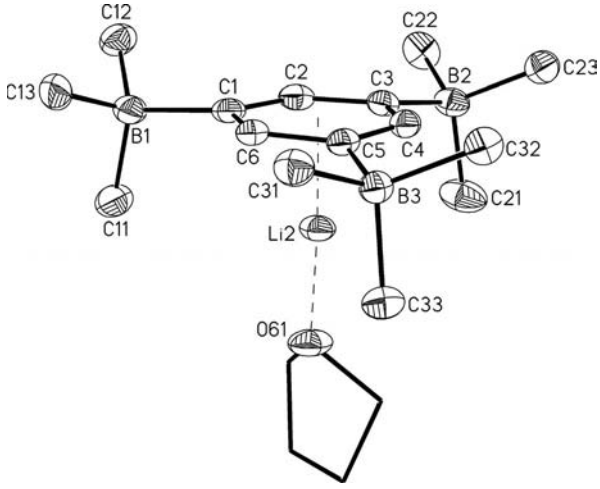

Figure 4. Molecular structure of $[\{Li(thf)\}\{\mathbf{10}\}]^{2-}$; displacement parameters are at 30% probability. H atoms are omitted for clarity. Selected bond lengths [Å] and angles [°]: Li(2)–O(61) 1.891(6), Li(2)–COG 1.784, B(1)–C(1) 1.645(6), B(2)–C(3) 1.644(6), B(3)–C(5) 1.635(6); Li(2)–COG–C(1) 90.6, Li(2)–COG–C(3) 89.6, Li(2)–COG–C(5) 89.3, COG–Li(2)–O(61) 176.4. COG: centroid of the C_6H_3 bridge.

Considering the pronounced structural differences between the di- and trianionic benzene derivatives $[Li(12\text{-}c\text{-}4)_2]_2$[**2**] and $[\{Li(12\text{-}c\text{-}4)_2\}_2Li(thf)]$[**10**], we decided to investigate the trianionic trihydridoborate Li_3[**12**] and compare its solid-state structure with that of its dianionic analogue $[Li(thf)_2]_2[m\text{-}C_6H_4(BH_3)_2]$.[35] Li_3[**12**] was readily accessed from the reaction between the boronic acid ester **11**[47,48] (Scheme 3) and 4.5 equivalents of $Li[AlH_4]$ in Et_2O. X-ray quality crystals were grown by diffusion of Et_2O into a dilute THF solution of Li_3[**12**].

The $^{11}B\{^1H\}$ NMR spectrum of Li_3[**12**] shows one resonance at –24.7 ppm, which splits into a quartet in the proton-coupled case ($^1J_{BH}$ = 78 Hz) {cf. $Li_2[C_6H_2(BH_3)_2(n\text{-hexyl})_2]$: $\delta(^{11}B)$ = –26.2 ppm; $^1J_{BH}$ = 75 Hz}.[35] Correspondingly, the BH_3 protons of Li_3[**12**] give rise to a quartet at 1.07 ppm in the ^1H NMR spectrum.

According to X-ray crystallography, the chemical composition of the single crystalline material was $[\{Li(thf)_2\}_2Li]$[**12**] (under vacuum, most of the coordinated THF molecules are lost as shown by NMR spectroscopy and combustion analysis). The individual $[C_6H_3(BH_3)_3]^{3-}$ moieties in $[\{Li(thf)_2\}_2Li]$[**12**] are linked to each other by bridging Li^+ ions, thereby forming an extended coordination network in the solid state (Figure 5 middle). This network is essentially a superposition of the solid-state structures of the linear coordination polymer $[Li(thf)_2]_2[m\text{-}C_6H_4(BH_3)_2]$[35] (horizontal direction; Figure 5 top) and the anionic fragment $[\{Li(thf)\}\{\mathbf{10}\}]^{2-}$ with one BH_3 substituent replacing the THF ligand (vertical direction; Figure 5 bottom). Thus, similar to $[\{Li(12\text{-}c\text{-}4)_2\}_2Li(thf)]$[**10**], one of the three lithium ions of $[\{Li(thf)_2\}_2Li]$[**12**] is involved in a cation–π interaction [i.e. Li(3), Figure 6]. The coordination mode of Li(3) to the C_6H_3 ring is again η^6 with Li(3)–C bond lengths from 2.314(3) to 2.374(3) Å and a Li(3)–COG distance of 1.871 Å. Li(1) and Li(2) are not involved in cation–π interactions. Each of these ions binds to two THF ligands and to two BH_3 substituents, which belong to different $[C_6H_3(BH_3)_3]^{3-}$ anions. The corresponding Li···B distances vary between 2.439(4) and 2.497(4) Å, which indicates η^2-coordinated trihydridoborate[35] ligands. Compared to these values, the Li(3)···B(3C) contact of 2.107(4) Å is much shorter and testifies to a η^3-RBH_3–Li[35] coordination mode.

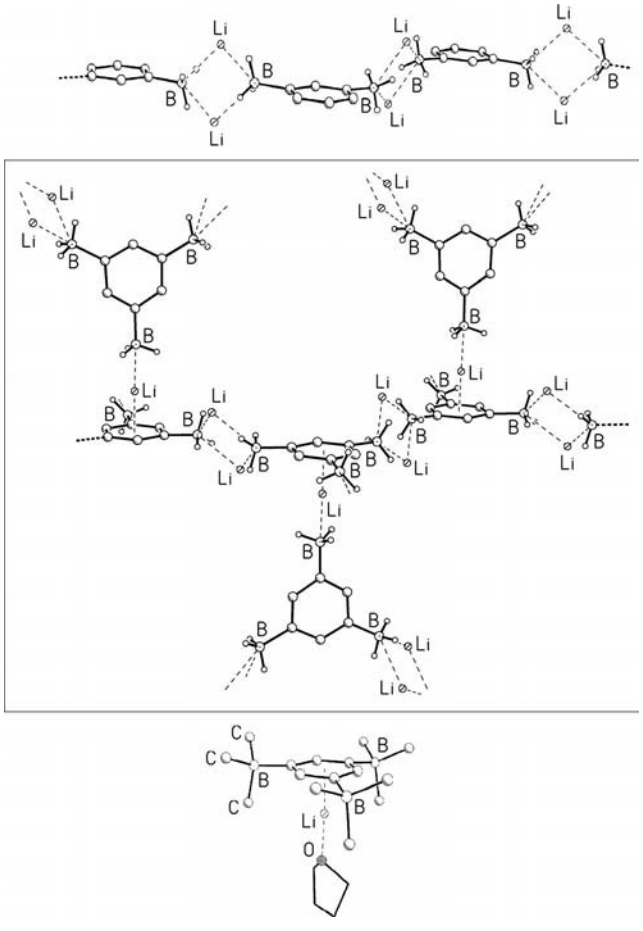

Figure 5. Comparison of key structural motifs of $[Li(thf)_2]_2[m\text{-}C_6H_4(BH_3)_2]$ (top), $[\{Li(thf)_2\}_2Li]$[**12**] (middle), and $[\{Li(12\text{-}c\text{-}4)_2\}_2Li(thf)]$[**10**] (bottom). Most H atoms and THF molecules are omitted for clarity.

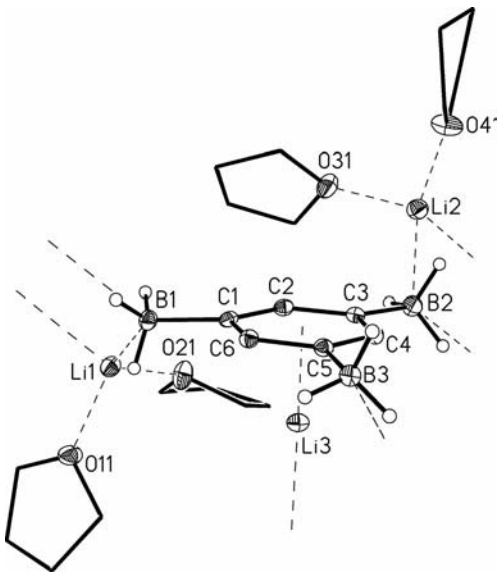

Figure 6. Molecular structure of the asymmetric unit of $[\{Li(thf)_2\}_2Li]$[**12**]; displacement parameters are at 50% probability. All H atoms attached to carbon atoms are omitted for clarity. Selected bond lengths [Å], atom···atom distances [Å], and bond angles [°]: Li(1)–O(11) 1.962(4), Li(1)–O(21) 2.012(4), Li(2)–O(31) 1.993(4), Li(2)–O(41) 1.948(4), Li(1)···B(1) 2.473(4), Li(1)···B(1A) 2.497(4), Li(2)···B(2) 2.495(4), Li(2)···B(2B) 2.439(4), Li(3)···B(3C) 2.107(4), Li(3)–COG 1.871; Li(3)–COG–C(1) 89.5, Li(3)–COG–C(3) 90.7, Li(3)–COG–C(5) 89.6, COG–Li(3)–B(3C) 177.6. Symmetry transformations used to generate equivalent atoms; A: $-x, -y + 1, -z + 1$; B: $-x + 1, -y + 1, -z + 1$; C: $x, -y + 3/2, z + 1/2$.

Conclusions

The solid-state structures of lithium salts have been investigated, in which the anion consists of a benzene ring equipped with one, two, or three $[-BR_3]^-$ substituents (R = H, Me, Ph). The aim was to promote cation–π interactions between Li^+ and the C_6H_5, p-C_6H_4, or 1,3,5-C_6H_3 fragment. The purpose of the anionic substituents was to assist the quadrupole moment of the aromatic fragment to attract Li^+ electrostatically.

The crystal structures of $[Li(thf)_4][(p\text{-}BrC_6H_4)BPh_3]$,[49] $[Li(thf)_2]_2[p\text{-}C_6H_4(BH_3)_2]$,[35] $[Li(12\text{-}c\text{-}4)_2]_2[p\text{-}C_6H_4(BMe_3)_2]$, $[Li(tetraglyme)]_2[p\text{-}C_6H_4(BPh_3)_2]$, and $[Li(thf)_3]_2[p\text{-}C_6H_4\{9\text{-}BBN(H)\}_2]$ all revealed fully solvent-separated ion pairs. This result clearly indicates that the attachment of one or two borate ions to a benzene molecule does not accumulate sufficient negative charge to attract a Li^+ cation to the π-

electron cloud of the aromatic ring − at least in the presence of strong donor solvents. In contrast, the solid-state structures of [{Li(12-c-4)$_2$}$_2$Li(thf)][1,3,5-$C_6H_3(BMe_3)_3$] and [{Li(thf)$_2$}$_2$Li][1,3,5-$C_6H_3(BH_3)_3$], which contain Li$^+$–benzene complexes, suggest that a benzene ring equipped with three negatively charged borate substituents presents a highly attractive π face to a Li$^+$ cation. Here, the cation–π interaction is inert towards THF and 12-c-4, which is one of the most potent Li$^+$ scavengers.

Experimental Section

General Considerations: All reactions were carried out under a N_2 atmosphere in carefully dried solvents using Schlenk tube techniques or a glove box. IR: Thermo Scientific Nicolet 6700 FT-IR spectrometer equipped with an ATR probe. NMR: Bruker Avance 300, Avance 400, and DPX 250. Chemical shift values (^{1}H, ^{13}C{^{1}H}) are reported in parts per million relative to $SiMe_4$ and were referenced to residual solvent signals. ^{11}B and ^{11}B{^{1}H} NMR spectra are referenced to external BF_3·Et_2O. *J* values are given in Hz. Abbreviations: s = singlet, d = doublet, q = quartet, n.r. = not resolved, n.o. = signal not observed. Elemental analyses were performed by the Microanalytical Laboratory of the University of Frankfurt or the Mikroanalytisches Labor Pascher, Remagen, Germany. Reagents purchased from commercial sources were used as received unless otherwise noted. 1,3,5-Tris(dibromoboryl)benzene (**9**)[37] and 1,3,5-tris(4,4,5,5-tetramethyl-1,3,2-dioxaborolan-2-yl)-benzene (**11**)[47,48] were prepared according to previously reported procedures.

Synthesis of Li$_2$[8]: To a suspension of **7** (1.34 g, 4.2 mmol) in THF (45 mL) at –78 °C was added a solution of *t*BuLi in pentane (4.4 mL, 8.4 mmol, 1.9 M) diluted with hexane (7 mL) dropwise over 20 min with stirring. The reaction mixture was warmed to room temp. overnight and the resulting clear solution was evaporated to dryness in vacuo to yield the crude product as a colorless powder (2.23 g). An analytically pure sample of [Li(dme)$_2$]$_2$[**8**] was obtained by gas-phase diffusion of pentane and hexane into a solution of the crude product in DME (14 mL) over a period of 7 d (on day 3, the sample was temporarily cooled to –30 °C in order to grow crystal seeds). The crystalline material obtained included X-ray quality crystals of [Li(dme)$_2$]$_2$[**8**]. Single crystals of [Li(thf)$_3$]$_2$[**8**] suitable for X-ray diffraction were grown by storing a solution of the crude product in THF/hexane at –30 °C for 1 d. Yield of [Li(dme)$_2$]$_2$[**8**]: 1.66 g (57%). IR (ATR probe): $\tilde{\nu}$ = 1915 [ν(BH)] cm^{-1}. ^{1}H NMR (400.1 MHz, [D$_8$]THF): δ = 7.28 (s, 4 H, C_6H_4-2,3,5,6), 1.98 (n.r., 6 H), 1.86 (n.r., 4 H), 1.78 (n.r., 6 H), 1.57 (n.r., 2 H), 1.43 (n.r., 4 H), 1.14 (n.r., 6 H, BBN-a,b,c), n.o. (B*H*) ppm. ^{13}C{^{1}H} NMR (100.6 MHz, [D$_8$]THF): δ = 133.7 (C_6H_4-2,3,5,6), 38.2 (BBN-b), 32.1 (BBN-b), 27.9 (BBN-c), 27.6 (BBN-c), n.o. (BBN-a, C_6H_4-1,4) ppm. ^{11}B{^{1}H} NMR (128.4 MHz, [D$_8$]THF): δ = –11.4 ($h_{1/2}$ = 60 Hz) ppm. ^{11}B{^{1}H} NMR (128.4 MHz, [D$_8$]THF): δ = –11.4 (d, $^1J_{BH}$ = 60 Hz) ppm. $C_{22}H_{34}B_2Li_2$·4($C_4H_{10}O_2$) (694.49): calcd. C 65.72, H 10.74; found C 65.84, H 10.56.

Synthesis of Li$_3$[10]: To a solution of 1,3,5-tris(dibromoboryl)benzene (6.21 g, 10.58 mmol) in toluene (30 mL) at –78 °C was added a solution of MeLi in Et_2O (59.5 mL, 95.2 mmol, 1.6 M) dropwise with vigorous stirring. After the addition was complete, stirring was continued for 30 min at –78 °C and for another 1 h at room temp. The resulting suspension was filtered, and the filtrate was evaporated to dryness in vacuo to yield a colorless solid (2.40 g, 88% assuming that no coordinated Et_2O remained). Single crystals of [{Li(12-c-4)$_2$}$_2$Li(thf)][**10**] suitable for X-ray diffraction analysis were obtained by gas-phase diffusion of Et_2O into a THF solution of the crude product in the presence of excess 12-c-4. ^{1}H NMR (400.1 MHz, [D$_6$]DMSO): δ = 6.78 (s, 3 H, C_6H_3-2,4,6), –0.54 (s, 27 H, CH_3) ppm. ^{13}C{^{1}H} NMR (62.9 MHz, [D$_6$]DMSO): δ = 130.3 (C_6H_3-2,4,6), 20.0 (q, $^1J_{BC}$ = 40 Hz, CH_3), n.o. (C_6H_3-1,3,5) ppm. ^{11}B{^{1}H} NMR (128.4 MHz, [D$_6$]DMSO): δ = –17.3 ($h_{1/2}$ = 30 Hz) ppm. $C_{15}H_{30}B_3Li_3$·4($C_8H_{16}O_4$)·C_4H_8O (1040.58): calcd. C 58.87, H 9.88; found C 58.55, H 9.78.

Synthesis of Li$_3$[12]: To a solution of **11** (1.29 g, 2.83 mmol) in Et_2O (35 mL) at –30 °C was added a solution of Li[AlH_4] in Et_2O (12.0 mL, 12.0 mmol, 1 M) dropwise with stirring over 30 min. Instant formation of a colorless precipitate was observed. The suspension was stirred at low temperature for 15 min, the cooling bath was removed, and stirring was continued overnight. The precipitate was collected on a frit and dried in vacuo. The solid was transferred into a Schlenk vessel, THF (50 mL) was added, and the resulting mixture was stirred for 2 h at room temp. and for 15 min at 40 °C. The slurry was allowed to cool to room temp., filtered, and the filtrate was evaporated to dryness under vacuum. The poorly soluble residue was washed with a mixture of Et_2O (10 mL) and THF (100 mL) and dried in vacuo. X-ray quality crystals of [{Li(thf)$_2$}$_2$-Li][**12**] were grown by gas-phase diffusion of Et_2O into a dilute THF solution of Li$_3$[**12**]. Yield of Li$_3$[**12**]·1/3(C_4H_8O) (combustion analysis): 0.36 g (79%). IR (ATR probe): $\tilde{\nu}$ = 2248, 2190 [ν(BH)] cm^{-1}. ^{1}H NMR (300.0 MHz, [D$_8$]THF): δ = 6.97 (s, 3 H, C_6H_3-2,4,6), 1.07 (q, $^1J_{BH}$ = 78 Hz, B*H*) ppm. ^{13}C{^{1}H} NMR (62.9 MHz, [D$_8$]THF): δ = 140.5 (C_6H_3-2,4,6), n.o. (C_6H_3-1,3,5) ppm. ^{11}B{^{1}H} NMR (96.3 MHz, [D$_8$]THF): δ = –24.7 ($h_{1/2}$ = 12 Hz) ppm. ^{11}B{^{1}H} NMR (96.3 MHz, [D$_8$]THF): δ = –24.7 (q, $^1J_{BH}$ = 78 Hz) ppm. $C_6H_{12}B_3Li_3$·1/3(C_4H_8O) (161.41): calcd. C 54.56, H 9.16; found C 54.81, H 9.23.

X-ray Crystal Structure Analyses of [Li(dme)$_2$]$_2$[8], [Li(thf)$_3$]$_2$[8], [{Li(12-c-4)$_2$}$_2$Li(thf)][10], and [{Li(thf)$_2$}$_2$Li][12]: Data collections were performed with a Stoe IPDS-II two-circle diffractometer with graphite-monochromated Mo-K_α radiation. Equivalent reflections were averaged. The structures were solved by direct methods[50] and refined with full-matrix least-squares on F^2 using the program SHELXL-97.[51] Unless noted otherwise, hydrogen atoms were placed in ideal positions and refined with fixed isotropic displacement parameters using a riding model (Tables 1 and 2).

The coordinates of H atoms bonded to B atoms in [Li(thf)$_3$]$_2$[**8**] were refined. One methylene group of a THF molecule in [Li(thf)$_3$]$_2$[**8**] is disordered over two sites with a site occupancy factor of 0.58(1) for the major occupied site. The disordered atoms were refined isotropically. The H atoms bonded to B atoms in [Li(dme)$_2$]$_2$[**8**] were freely refined. Two crown ether rings and two C atoms of the THF molecule in [{Li(12-c-4)$_2$}$_2$Li(thf)][**10**] are disordered over two sites with site occupancy factors of 0.505(7), 0.527(7), and 0.554(9), respectively, for the major occupied sites. Bond lengths were restrained to keep the geometric parameters of the disordered moieties in a reasonable range.

CCDC-832428 {for [Li(12-c-4)$_2$]$_2$[**2**]}, -832430 {for [Li(dme)$_3$][**4**]}, -832429 {for [Li(thf)$_4$][**4**]}, -832424 {for [Li(thf)$_4$]$_2$[**5**]}, -832431 {for [Li(tetraglyme)]$_2$[**5**]}, -832432 (for **7**), -832427 {for [Li(dme)$_2$]$_2$[**8**]}, -832426 {for [Li(thf)$_3$]$_2$[**8**]}, -832423 {for [{Li(12-c-4)$_2$}$_2$Li-(thf)][**10**]}, and -832425 {for [{Li(thf)$_2$}$_2$Li][**12**]} contain the supplementary crystallographic data for this paper. These data can be obtained free of charge from The Cambridge Crystallographic Data Centre via www.ccdc.cam.ac.uk/data_request/cif.

Table 1. Crystal data and structure refinement details for [{Li(dme)$_2$}$_2${**8**}]$_2$ and [Li(thf)$_3$]$_2$[**8**].

	[{Li(dme)$_2$}$_2${**8**}]$_2$	[Li(thf)$_3$]$_2$[**8**]
Formula	$C_{76}H_{148}B_4Li_4O_{16}$	$C_{46}H_{82}B_2Li_2O_6$
Fw	1388.94	766.62
Color, shape	colorless, plate	colorless, plate
Temperature [K]	173(2)	173(2)
Radiation	Mo-K_α, 0.71073 Å	Mo-K_α, 0.71073 Å
Crystal system	monoclinic	monoclinic
Space group	$P2_1/c$	$P2_1/n$
a [Å]	9.3822(4)	10.6092(9)
b [Å]	25.7590(8)	11.5236(7)
c [Å]	17.6520(8)	19.2827(16)
α [°]	90	90
β [°]	93.141(3)	97.493(7)
γ [°]	90	90
V [Å^3]	4259.7(3)	2337.3(3)
Z	2	2
$D_{calcd.}$ [g cm^{-3}]	1.083	1.089
F(000)	1528	844
μ [mm^{-1}]	0.071	0.068
Crystal size [mm]	0.35 × 0.35 × 0.21	0.80 × 0.50 × 0.50
Reflections collected	53345	18450
Indep. reflections (R_{int})	8297 (0.0817)	4599 (0.0849)
Data/restraints/parameters	8297/0/460	4599/0/257
GOOF on F^2	1.001	1.083
$R1$, $wR2$ [$I > 2\sigma(I)$]	0.0406, 0.1022	0.0741, 0.2185
$R1$, $wR2$ (all data)	0.0556, 0.1082	0.0983, 0.2363
Largest diff. peak and hole [e Å^{-3}]	0.251 and –0.182	0.427 and –0.236

Table 2. Crystal data and structure refinement details for [{Li(12-c-4)$_2$}$_2$Li(thf)][**10**] and [{Li(thf)$_2$}$_2$Li][**12**].

	[{Li(12-c-4)$_2$}$_2$-Li(thf)][**10**]	[{Li(thf)$_2$}$_2$Li][**12**]
Formula	$C_{51}H_{102}B_3Li_3O_{17}$	$C_{22}H_{44}B_3Li_3O_4$
Fw	1040.58	425.82
Color, shape	colorless, block	colorless, block
Temperature [K]	100(2)	173(2)
Radiation	Mo-K_α, 0.71073 Å	Mo-K_α, 0.71073 Å
Crystal System	monoclinic	monoclinic
Space group	$P2_1/n$	$P2_1/c$
a [Å]	19.9648(14)	15.0006(12)
b [Å]	13.5601(14)	18.4160(14)
c [Å]	24.0737(17)	9.6928(8)
α [°]	90	90
β [°]	113.062(5)	93.736(6)
γ [°]	90	90
V [Å^3]	5996.5(9)	2672.0(4)
Z	4	4
$D_{calcd.}$ [g cm^{-3}]	1.153	1.059
F(000)	2272	928
μ [mm^{-1}]	0.082	0.065
Crystal size [mm]	0.44 × 0.43 × 0.37	0.19 × 0.05 × 0.05
Reflections collected	57572	13769
Indep. reflections (R_{int})	10960 (0.0623)	5003 (0.0405)
Data/restraints/parameters	10960/77/907	5003/0/292
GOOF on F^2	0.872	1.044
$R1$, $wR2$ [$I > 2\sigma(I)$]	0.0955, 0.2646	0.0638, 0.1721
$R1$, $wR2$ (all data)	0.1632, 0.3008	0.0773, 0.1816
Largest diff. peak and hole [e Å^{-3}]	0.830 and –0.404	0.361 and –0.326

Some details of the X-ray crystal structure analyses of [Li(12-c-4)$_2$]$_2$[**2**], [Li(dme)$_3$][**4**], [Li(thf)$_4$][**4**], [Li(thf)$_4$]$_2$[**5**], [Li(tetraglyme)]$_2$[**5**], and **7** are also provided in the Supporting Information.

Supporting Information (see footnote on the first page of this article): Syntheses of Li_2[**2**], Li[**4**], Li_2[**5**], and **7**. X-ray crystal structure analyses of [Li(12-c-4)$_2$]$_2$[**2**], [Li(dme)$_3$][**4**], [Li(thf)$_4$][**4**], [Li(thf)$_4$]$_2$[**5**], [Li(tetraglyme)]$_2$[**5**], and **7**.

Acknowledgments

M. W. acknowledges financial support by the Beilstein Institut, Frankfurt/Main, Germany, within the research collaboration NanoBiC.

[1] C. Elschenbroich, *Organometallics*, 3rd ed., Wiley-VCH, Weinheim, Germany, **2006**.
[2] J. C. Ma, D. A. Dougherty, *Chem. Rev.* **1997**, *97*, 1303–1324.
[3] G. W. Gokel, S. L. De Wall, E. S. Meadows, *Eur. J. Org. Chem.* **2000**, 2967–2978.
[4] G. W. Gokel, L. J. Barbour, S. L. De Wall, E. S. Meadows, *Coord. Chem. Rev.* **2001**, *222*, 127–154.
[5] G. W. Gokel, L. J. Barbour, R. Ferdani, J. Hu, *Acc. Chem. Res.* **2002**, *35*, 878–886.
[6] G. H. Posner, C. M. Lentz, *J. Am. Chem. Soc.* **1979**, *101*, 934–946.
[7] C. A. Broka, T. Shen, *J. Am. Chem. Soc.* **1989**, *111*, 2981–2984.
[8] W. F. Bailey, A. D. Khanolkar, K. Gavaskar, T. V. Ovaska, K. Rossi, Y. Thiel, K. B. Wiberg, *J. Am. Chem. Soc.* **1991**, *113*, 5720–5727.
[9] L. S. Kaanumalle, J. Sivaguru, N. Arunkumar, S. Karthikeyan, V. Ramamurthy, *Chem. Commun.* **2003**, 116–117.
[10] P. Monje, M. R. Paleo, L. García-Río, F. J. Sardina, *J. Org. Chem.* **2008**, *73*, 7394–7397.
[11] L. M. Salonen, M. Ellermann, F. Diederich, *Angew. Chem.* **2011**, *123*, 4908–4944; *Angew. Chem. Int. Ed.* **2011**, *50*, 4808–4842.
[12] M. Yoshio, R. J. Brodd, A. Kozawa, *Lithium-Ion Batteries*, Springer, Berlin, **2009**.
[13] a) J. J. Brooks, W. Rhine, G. D. Stucky, *J. Am. Chem. Soc.* **1972**, *94*, 7346–7351; b) C. Melero, A. Guijarro, M. Yus, *Dalton Trans.* **2009**, 1286–1289. Another particularly revealing example is the inverse double-decker sandwich complex [Li(thf)$_2$]$_2$-[$C_{12}H_{10}B_2$] because its dianionic π system is formally isoelectronic to neutral anthracene: c) A. Lorbach, M. Bolte, H.-W. Lerner, M. Wagner, *Organometallics* **2010**, *29*, 5762–5765.
[14] For selected examples, see: a) M. Niemeyer, P. P. Power, *Inorg. Chem.* **1996**, *35*, 7264–7272; b) S. Horchler, E. Parisini, H. W. Roesky, H.-G. Schmidt, M. Noltemeyer, *J. Chem. Soc., Dalton Trans.* **1997**, 2761–2763; c) X.-W. Li, J. Su, G. H. Robinson, *Chem. Commun.* **1998**, 1281–1282; d) G. Mund, D. Vidovic, R. J. Batchelor, J. F. Britten, R. D. Sharma, C. H. W. Jones, D. B. Leznoff, *Chem. Eur. J.* **2003**, *9*, 4757–4763; e) B. E. Eichler, A. D. Phillips, P. P. Power, *Organometallics* **2003**, *22*, 5423–5426; f) S. Bieller, F. Zhang, M. Bolte, J. W. Bats, H.-W. Lerner, M. Wagner, *Organometallics* **2004**, *23*, 2107–2113; g) A. Rodriguez-Delgado, E. Y.-X. Chen, *J. Am. Chem. Soc.* **2005**, *127*, 961–974; h) C. Ni, J. C. Fettinger, G. J. Long, P. P. Power, *Dalton Trans.* **2010**, *39*, 10664–10670.
[15] Donor-free unsubstituted fluorenyllithium features π-bonded Li^+ ions only. The lattice is built of cyclic dimers, in which each of the two Li^+ ions is encapsulated between two six-membered rings: C. Üffing, R. Köppe, H. Schnöckel, *Organometallics* **1998**, *17*, 3512–3515.
[16] R. E. Dinnebier, U. Behrens, F. Olbrich, *J. Am. Chem. Soc.* **1998**, *120*, 1430–1433.
[17] A. Hübner, T. Bernert, I. Sänger, E. Alig, M. Bolte, L. Fink, M. Wagner, H.-W. Lerner, *Dalton Trans.* **2010**, *39*, 7528–7533.

[18] K. Ruhlandt-Senge, J. J. Ellison, R. J. Wehmschulte, F. Pauer, P. P. Power, *J. Am. Chem. Soc.* **1993**, *115*, 11353–11357.
[19] R. P. Davies, S. Hornauer, A. J. P. White, *Chem. Commun.* **2007**, 304–306.
[20] A. Fürstner, R. Martin, H. Krause, G. Seidel, R. Goddard, C. W. Lehmann, *J. Am. Chem. Soc.* **2008**, *130*, 8773–8787.
[21] B. Schiemenz, P. P. Power, *Angew. Chem.* **1996**, *108*, 2288–2290; *Angew. Chem. Int. Ed. Engl.* **1996**, *35*, 2150–2152.
[22] T. Fukawa, M. Nakamoto, V. Y. Lee, A. Sekiguchi, *Organometallics* **2004**, *23*, 2376–2381.
[23] M. Bolte, I. Ruderfer, T. Müller, *Acta Crystallogr., Sect. E* **2005**, *61*, m1581–m1582.
[24] S. Scholz, J. C. Green, H.-W. Lerner, M. Bolte, M. Wagner, *Chem. Commun.* **2002**, 36–37.
[25] A. Haghiri Ilkhechi, M. Scheibitz, M. Bolte, H.-W. Lerner, M. Wagner, *Polyhedron* **2004**, *23*, 2597–2604.
[26] A. Haghiri Ilkhechi, M. Bolte, H.-W. Lerner, M. Wagner, *J. Organomet. Chem.* **2005**, *690*, 1971–1977.
[27] L. Kaufmann, A. Haghiri Ilkhechi, H. Vitze, M. Bolte, H.-W. Lerner, M. Wagner, *J. Organomet. Chem.* **2009**, *694*, 466–472.
[28] A. Haghiri Ilkhechi, J. M. Mercero, I. Silanes, M. Bolte, M. Scheibitz, H.-W. Lerner, J. M. Ugalde, M. Wagner, *J. Am. Chem. Soc.* **2005**, *127*, 10656–10666.
[29] L. Kaufmann, H. Vitze, M. Bolte, H.-W. Lerner, M. Wagner, *Organometallics* **2007**, *26*, 1771–1776.
[30] D. Vagedes, G. Kehr, D. König, K. Wedeking, R. Fröhlich, G. Erker, C. Mück-Lichtenfeld, S. Grimme, *Eur. J. Inorg. Chem.* **2002**, 2015–2021.
[31] K. Kunz, F. Blasberg, M. Bolte, H.-W. Lerner, M. Wagner, *Inorg. Chim. Acta* **2009**, *362*, 4372–4376.
[32] L. Kaufmann, J.-M. Breunig, H. Vitze, F. Schödel, I. Nowik, M. Pichlmaier, M. Bolte, H.-W. Lerner, R. F. Winter, R. H. Herber, M. Wagner, *Dalton Trans.* **2009**, 2940–2950.
[33] M. Nanjo, K. Matsudo, M. Kurihara, S. Nakamura, Y. Sakaguchi, H. Hayashi, K. Mochida, *Organometallics* **2006**, *25*, 832–838.
[34] For selected examples of corresponding Li^+ complexes, see: a) W. J. Evans, T. J. Boyle, J. W. Ziller, *Organometallics* **1992**, *11*, 3903–3907; b) S. Harder, M. H. Prosenc, *Angew. Chem.* **1994**, *106*, 1830–1832; *Angew. Chem. Int. Ed. Engl.* **1994**, *33*, 1744–1746; c) M. Könemann, G. Erker, M. Grehl, R. Fröhlich, E.-U. Würthwein, *J. Am. Chem. Soc.* **1995**, *117*, 11215–11219; d) C. Dohmeier, E. Baum, A. Ecker, R. Köppe, H. Schnöckel, *Organometallics* **1996**, *15*, 4702–4706; e) K. Kunz, J. Pflug, A. Bertuleit, R. Fröhlich, E. Wegelius, G. Erker, E.-U. Würthwein, *Organometallics* **2000**, *19*, 4208–4216; f) W. Nie, C. Qian, Y. Chen, J. Sun, *Organometallics* **2001**, *20*, 5780–5783; g) G. R. Giesbrecht, J. C. Gordon, D. L. Clark, B. L. Scott, *Dalton Trans.* **2003**, 2658–2665; h) C. Fernández-Cortabitarte, F. García, J. V. Morey, M. McPartlin, S. Singh, A. E. H. Wheatley, D. S. Wright, *Angew. Chem.* **2007**, *119*, 5521–5523; *Angew. Chem. Int. Ed.* **2007**, *46*, 5425–5427; i) V. V. Kotov, C. Wang, G. Kehr, R. Fröhlich, G. Erker, *Organometallics* **2007**, *26*, 6258–6262.
[35] D. Franz, M. Bolte, H.-W. Lerner, M. Wagner, *Dalton Trans.* **2011**, *40*, 2433–2440.
[36] M. Scheibitz, H. Li, J. Schnorr, A. Sánchez Perucha, M. Bolte, H.-W. Lerner, F. Jäkle, M. Wagner, *J. Am. Chem. Soc.* **2009**, *131*, 16319–16329.
[37] M. C. Haberecht, J. B. Heilmann, A. Haghiri, M. Bolte, J. W. Bats, H.-W. Lerner, M. C. Holthausen, M. Wagner, *Z. Anorg. Allg. Chem.* **2004**, *630*, 904–913.
[38] Comparable lithium–halogen exchange reactions on brominated arylborate anions have been described: a) G. A. Molander, N. M. Ellis, *J. Org. Chem.* **2006**, *71*, 7491–7493; b) Q. Jiang, M. Ryan, P. Zhichkin, *J. Org. Chem.* **2007**, *72*, 6618–6620.
[39] Z. Bao, W. K. Chan, L. Yu, *J. Am. Chem. Soc.* **1995**, *117*, 12426–12435.
[40] H. C. Brown, S. U. Kulkarni, *J. Organomet. Chem.* **1979**, *168*, 281–293.
[41] H. C. Brown, G. W. Kramer, J. L. Hubbard, S. Krishnamurthy, *J. Organomet. Chem.* **1980**, *188*, 1–10.
[42] R. Köster, G. Seidel, K. Wagner, B. Wrackmeyer, *Chem. Ber.* **1993**, *126*, 305–317.
[43] R. A. Kumpf, D. A. Dougherty, *Science* **1993**, *261*, 1708–1710.
[44] H. Nöth, B. Wrackmeyer, *Nuclear Magnetic Resonance Spectroscopy of Boron Compounds*, in: *NMR Basic Principles and Progress* (Eds.: P. Diehl, E. Fluck, R. Kosfeld), Springer, Berlin, **1978**.
[45] D. Feller, D. A. Dixon, J. B. Nicholas, *J. Phys. Chem. A* **2000**, *104*, 11414–11419.
[46] J. C. Amicangelo, P. B. Armentrout, *J. Phys. Chem. A* **2000**, *104*, 11420–11432.
[47] A. B. Morgan, J. L. Jurs, J. M. Tour, *J. Appl. Polym. Sci.* **2000**, *76*, 1257–1268.
[48] L. H. Tong, S. I. Pascu, T. Jarrosson, J. K. M. Sanders, *Chem. Commun.* **2006**, 1085–1087.
[49] A number of solvent-separated ion pairs $[Li(solv)_n][BPh_4]$ containing the parent tetraphenylborate ion have also been structurally characterized: a) P. K. Bakshi, S. V. Sereda, O. Knop, M. Falk, *Can. J. Chem.* **1994**, *72*, 2144–2152; b) H. Schödel, T. Vaupel, H. Bock, *Acta Crystallogr., Sect. C* **1996**, *52*, 637–640; c) J. M. Butler, G. M. Gray, *J. Chem. Crystallogr.* **2002**, *32*, 171–175; d) W. A. Henderson, N. R. Brooks, W. W. Brennessel, V. G. Young Jr., *Chem. Mater.* **2003**, *15*, 4679–4684; e) W. A. Henderson, N. R. Brooks, V. G. Young Jr., *J. Am. Chem. Soc.* **2003**, *125*, 12098–12099.
[50] G. M. Sheldrick, *Acta Crystallogr., Sect. A* **1990**, *46*, 467–473.
[51] G. M. Sheldrick, *SHELXL-97. A Program for the Refinement of Crystal Structures*, Universität Göttingen, Germany, **1997**.

Received: August 3, 2011
Published Online: November 15, 2011

